

**Figure 4.** Kinetic energy dependence of the contribution of the representative point for the rate constant of O-H insertion at 77 K. Abcissa: Kinetic energy of the representative point. Ordinate: The normalized values of the tunneling probability  $P(E_T)$  (---), Boltzmann distribution  $\exp(-E_T/kT)$  (-·-·-), and their product  $P(E_T) \exp(-E_T/kT)$  (—). The normalization was carried out such that the maximum of each of these values is 1. The reaction rate constant is obtained by the integration of the area below the solid curve (see formula 3).

conclusion is obtained by the classical mechanism as well as the tunneling mechanism (Figure 3). However, the very low activation energy at low temperatures<sup>2,3,9</sup> can be explained by the tunneling mechanism only as found in Figure 3.

The isotope effect in tunneling is explained by the increase of the effective thickness of the potential energy barrier along the IRC path as well as the increase of the effective barrier height.<sup>22</sup> Recent observations of the isotope effect in the same reaction at

low temperature<sup>23</sup> may be explained by the treatment considering these origins.

**Contribution of Hydrogen Atom Displacement to the Tunneling Effect.** The unique normal mode of vibration of imaginary frequency at the saddle point is shown in Figure 2 for each of the reactions investigated. It is interesting that the normal mode of vibration of imaginary frequency is the displacement of the bridged hydrogen atom only in all of the reactions.

Le Roy used the mass of the hydrogen atom being abstracted as the effective reduced mass of the reacting system  $\cdot\text{CH}_3 + \text{CH}_3\text{CN} \rightarrow \text{CH}_4 + \cdot\text{CH}_2\text{CN}$  in tunneling.<sup>6</sup> Brunton et al. used the same treatment in their publication.<sup>9</sup> If the bridged hydrogen atom displacement only would be the main contribution to tunneling also in the present research, the tunneling passing through the energy barrier must be done by the representative point whose translational energy is nearly equal to  $V(Q_m)$ , because the main contribution of the bridged hydrogen atom displacement is only effective near  $Q_m$  in Figure 1. However, this consideration is wrong as is clearly shown in Figure 4, as an example, where the main contribution to the rate constant is due to the tunneling of the representative point whose translational energy is very low. This means that the reaction system follows approximately the whole structure change along the IRC path even when the tunneling takes place at the low temperature; i.e., the displacements of not only the bridged hydrogen atom but also all of the atoms constructing the reaction system contribute to the tunneling as well as to the classical mechanism.

**Acknowledgment.** The authors thank the Computer Center, Institute for Molecular Science, Okazaki, for the use of the M-200H computer and the Library programs GAUSSIAN80 and GAMESS. The computation was also carried out at the Computer Center, the University of Tokyo, and the Computer Center, Chiba University.

**Registry No.** Methylene, 2465-56-7; methanol, 67-56-1.

(22) M. Tsuda, S. Oikawa, and K. Nagayama, Symposium on Photochemistry (Japanese), 1983, Tsukuba (1983), p 369.

(23) H. Tomioka, Y. Ozaki, and Y. Izawa, *Bull. Chem. Soc. Jpn.*, **56**, 1239 (1983).

## Solid-State NMR of Cyclic Pentapeptides

M. H. Frey,<sup>†</sup> S. J. Opella,<sup>\*†</sup> A. L. Rockwell,<sup>†</sup> and L. M. Gierasch<sup>\*†</sup>

*Contribution from the Departments of Chemistry, University of Pennsylvania, Philadelphia, Pennsylvania 19104, and University of Delaware, Newark, Delaware 19711.*

*Received July 23, 1984*

**Abstract:** The structure and dynamics of several cyclic pentapeptides with well-defined conformational features are described by solid-state NMR spectroscopy. Isotropic chemical shift spectra for solution and polycrystalline samples are compared. The dynamics of phenyl ring side chains are described with line-shape analysis of both high-resolution spectra and powder patterns. The bond lengths of N-H groups involved in intramolecular hydrogen bonds are measured.

Solid-state NMR spectroscopy is an effective way to describe the structural and dynamical properties of crystalline and amorphous solid biological molecules.<sup>1</sup> NMR studies provide structural information that is complementary to that obtained from diffraction studies. For those molecules that do not form single crystals or are insoluble, solid-state NMR spectroscopy provides one of the few ways of studying these molecules at high resolution. For those molecules that form single crystals suitable for X-ray or neutron diffraction studies, solid-state NMR spectroscopy

provides unique dynamical information and complementary structural information. Synthetic cyclic peptides serve as interesting and convenient model systems for exploring applications of solid-state NMR to biological systems. The general spectroscopic approach is appropriate for essentially any medium-sized molecule, and some features of it can be extended to macromolecules. We have concentrated on polycrystalline samples; although alternative strategies that utilize the spectroscopic properties of single crystals are in some cases more powerful, they

<sup>†</sup>University of Pennsylvania.

<sup>\*</sup>University of Delaware.

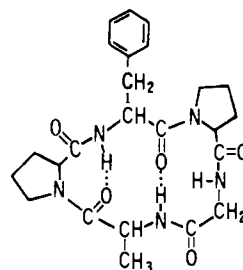
(1) Opella, S. J. *Annu. Rev. Phys. Chem.* **1982**, *33*, 533-562.

are generally limited by practical aspects of sample preparation.

We have identified our general categories of solid-state NMR experiments that are useful in obtaining structural information on polycrystalline samples of peptides. (1) The simplest and most readily applied utilizes  $^{13}\text{C}$  isotropic chemical shifts as an empirical parameter indicative of local conformational features. In favorable cases, the chemical shifts can be used to make direct comparisons between solid-state and solution conformation.<sup>2,3</sup> (2) Considerable experimental and theoretical efforts have been devoted to understanding the influence of  $^{14}\text{N}$  on  $^{13}\text{C}$  resonance properties.<sup>4-8</sup> Since the spectral effects of nitrogen on the resonances of bonded carbons are dependent on distance and angular factors, the line shapes of the carbon resonances can be used as a source of structural information about peptide bonds. (3) The dipole-dipole coupling between bonded atoms gives a direct measurement of bond length with high precision<sup>9</sup> and can be determined in powder samples,<sup>10,11</sup> this is illustrated here for the N-H bonds involved in intramolecular hydrogen bonds in cyclic peptides. (4) Recent  $^{13}\text{C}$  spin-exchange experiments have been able to identify carbon sites that are close in space<sup>12</sup> and have the potential for providing a general method of structure determination.

Dynamics of amino acids, peptides, and proteins in the solid state have been the subject of investigations in several laboratories by solid-state NMR.<sup>13</sup> This approach to characterizing molecular dynamics benefits from the possibilities for direct line-shape analysis and the absence of overall reorientation for molecules in the solid state. There are three types of NMR measurements used to describe molecular dynamics. (1) In the isotropic chemical shift spectra obtained with magic angle sample spinning, line multiplicities and line shapes reflect some averaging processes on a relatively slow time scale. (2) The detailed analysis of powder pattern line shapes is a powerful approach for characterizing rapid, large amplitude motions in immobilized molecules. (3) Relaxation measurements provide quantitative rate information, especially when the amplitudes and directions of motions are established from line-shape analysis.

Cyclic pentapeptides have been studied extensively by a variety of physical methods, especially NMR spectroscopy.<sup>14,15</sup> These peptides have been found to have rigid and well-defined conformations in solution and in crystals.<sup>16,17</sup> Therefore, they serve as models to demonstrate the relationships between amino acid sequence and three-dimensional conformations as well as for the development of the solid-state NMR spectroscopy.<sup>3,5,12,18-20</sup> The



Cyclic (D-Phe-Pro-Gly-D-Ala-Pro)

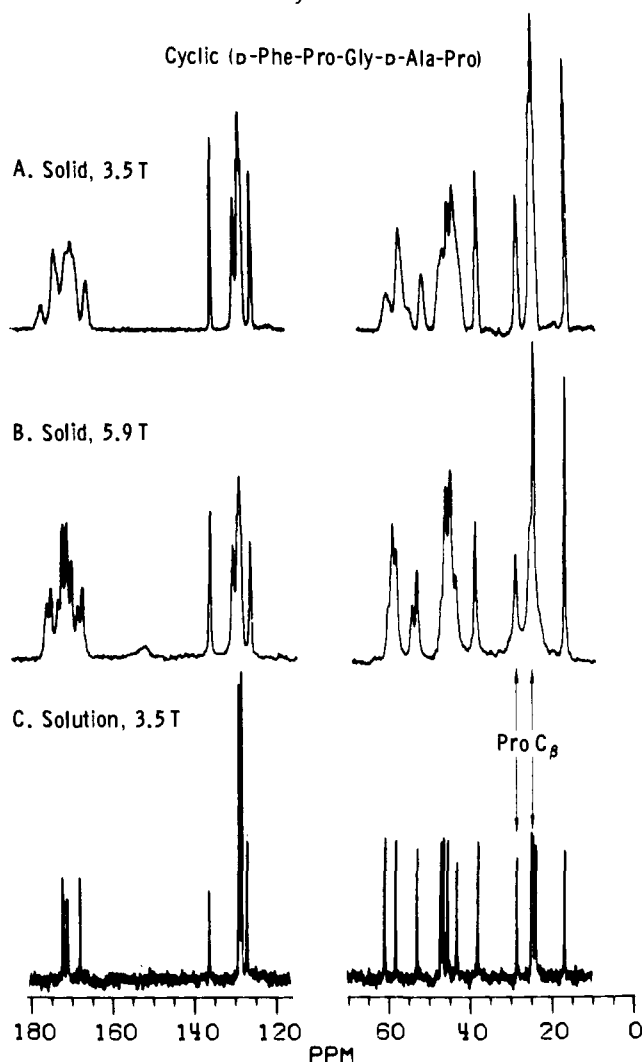


**Figure 1.** High-resolution  $^{13}\text{C}$  NMR spectra of cyclic (D-Phe-Pro-Gly-D-Ala-Pro). (A) Solid-state NMR spectrum at 3.5 T obtained with 12 800 single cross-polarization acquisitions with 2.5-mT decoupling and 5-s recycle delay. The 120–180 ppm region was obtained at a 2.4-kHz spin rate in a Kel-F rotor while the 0–70 ppm region was obtained at a 3.1-kHz spin rate in a Delrin rotor. (B) Solid-state NMR spectrum at 5.9 T obtained with 13 800 single cross-polarization acquisitions with 1.5-mT decoupling, 3-s recycle delay, and 4.0-kHz spin rate in a Delrin rotor. (C) Solution NMR spectrum at 3.5 T of a 20-mg/mL  $\text{CDCl}_3/\text{CD}_3\text{OD}$  solution.

cyclic pentapeptides used in the studies described in this paper adopt all-trans solution conformations which contain reverse turns. Both  $\beta$  turns (involving four residues) and  $\gamma$  turns (involving three residues) can be present, depending on the sequence of the peptide.

(2) Frey, M. H.; Opella, S. J. *J. Chem. Soc., Chem. Commun.* **1980**, 474–475.

(3) Pease, L. G.; Frey, M. H.; Opella, S. J. *J. Am. Chem. Soc.* **1981**, *103*, 467–498.

(4) Hexem, J. G.; Frey, M. H.; Opella, S. J. *J. Am. Chem. Soc.* **1981**, *103*, 224–226.

(5) Opella, S. J.; Hexem, J. G.; Frey, M. H.; Cross, T. A. *Philos. Trans. R. Soc. London, Ser. A* **1981**, *299*, 665–683.

(6) Hexem, J. G.; Frey, M. H.; Opella, S. J. *J. Chem. Phys.* **1982**, *77*, 3847–3856.

(7) Naito, A.; Ganapathy, S.; McDowell, C. A. *J. Chem. Phys.* **1981**, *74*, 5393–5398.

(8) Zumbulyadis, N.; Henrichs, P. M.; Young, R. H. *J. Chem. Phys.* **1981**, *75*, 1603–1611.

(9) Apke, G. *J. Chem. Phys.* **1948**, *16*, 327–336.

(10) Munowitz, M. G.; Griffin, R. G.; Bodenhausen, G.; Huang, T. H. *J. Am. Chem. Soc.* **1981**, *103*, 2529–2533.

(11) DiVerdi, J. A.; Opella, S. J. *J. Am. Chem. Soc.* **1982**, *104*, 1761–1762.

(12) Frey, M. H.; Opella, S. J. *J. Am. Chem. Soc.* **1984**, *106*, 4942–4945.

(13) Reviewed in: Opella, S. *J. Methods Enzymol.*, in press.

(14) Pease, L. G. in "Peptides: Structure and Biological Function: Proceedings of the 6th American Peptide Symposium; Gross, E., Meienhofer, J., Eds., Pierce Chem. Co.: Rockford, IL, 1979; pp 197–200.

(15) Pease, L. G.; Watson, C. *J. Am. Chem. Soc.* **1979**, *101*, 1279–1286.

(16) Karle, I. L. *J. Am. Chem. Soc.* **1978**, *100*, 1286–1289.

(17) Karle, I. L. *J. Am. Chem. Soc.* **1979**, *101*, 181–184.

(18) Gierasch, L. M.; Frey, M. H.; Hexem, J. G.; Opella, S. J. in "New Methods and Applications of NMR Spectroscopy"; Levy, G., Ed.; American Chemical Society: Washington, D.C., 1982; pp 233–247.

(19) Gierasch, L. M.; Opella, S. J.; Frey, M. H. in "Peptides: Synthesis, Structure and Function: Proceedings of the 7th American Peptide Symposium"; Rich, D. H., Gross, E., Eds.; Pierce Chem. Co.: Rockford, IL, 1981; pp 267–276.

(20) Frey, M. H.; Hexem, J. G.; Leo, G. C.; Tsang, P.; Opella, S. J.; Rockwell, A. L.; Gierasch, L. M. in "Peptides: Structure and Function: Proceedings of the 8th American Peptide Symposium; Hruby, V. J., Rich, D. H., Eds.; Pierce Chem. Co.: Rockford, IL, 1983; pp 763–771.

It can be concluded from the previous studies of these peptides<sup>14</sup> that a  $\gamma$  turn with significant hydrogen bonding is a general feature of the proline-containing cyclic pentapeptides. There is considerable variability in the  $\beta$ -turn portion of these molecules, and it is not always hydrogen bonded.

This paper summarizes the general features of the applications of NMR spectroscopy to crystalline cyclic pentapeptides. Structural and dynamical aspects of three cyclic pentapeptides are compared. Each of the spectroscopic experiments is described in detail elsewhere.

### Experimental Section

The solid-state NMR experiments were performed on home-built double-resonance spectrometers with 3.5- and 5.9-T magnetic fields. The isotropic chemical shift  $^{13}\text{C}$  and  $^{15}\text{N}$  NMR spectra were obtained at both field strengths by cross-polarization with magic angle sample spinning and proton decoupling for line narrowing. The  $^2\text{H}$  NMR spectra were obtained at 5.9 T with the quadrupole echo pulse sequence with an interpulse delay of 50  $\mu\text{s}$ . The two-dimensional  $^{15}\text{N}/^1\text{H}$  separated local field spectra were obtained as described previously<sup>11</sup> with "magic angle" proton decoupling<sup>21</sup> during the  $t_1$  evolution period.

The cyclic peptides were synthesized by solution methods described previously.<sup>15</sup> Detailed descriptions of the syntheses will be reported elsewhere. The  $^{15}\text{N}$ -labeled amino acid precursors were from KOR isotopes and the  $^2\text{H}$ -labeled phenylalanine was prepared as described previously.<sup>22</sup> The recrystallization of cyclic (D-Phe-Gly-Ala-Gly-Pro) was carried out by slow evaporation from methanol solution. The multiple crystal forms were found in a sample obtained by rapid recrystallization from methanol at elevated temperature. Other peptides were crystallized from methanol/ether solutions, and all of the peptide samples were in the form of small needle-like crystals.

### Results

**A. High-Resolution  $^{13}\text{C}$  NMR Spectra. (1) Cyclic (D-Phe-Pro-Gly-D-Ala-Pro).** High-resolution  $^{13}\text{C}$  NMR spectra of cyclic (D-Phe<sup>1</sup>-Pro<sup>2</sup>-Gly<sup>3</sup>-D-Ala<sup>4</sup>-Pro<sup>5</sup>) are shown in Figure 1. The spectra from solution and polycrystalline samples are compared, and the effects of magnetic field strength on the appearance of solid-state NMR spectra are demonstrated in the figure. The spectra in parts A and B of Figure 1 have been interpreted previously<sup>3</sup> as showing that the structure of cyclic (D-Phe-Pro-Gly-D-Ala-Pro) is the same in crystals and solution by virtue of the very high degree of correlation in the isotropic chemical shift frequencies in the two states. This correspondence of chemical shifts is generally not observed for conformationally flexible molecules.<sup>2</sup> This peptide has both  $\beta$  and  $\gamma$  turns stabilized by intramolecular hydrogen bonds.<sup>23</sup> As a consequence, the two proline residues have very different conformations. In particular, the proline in the  $\gamma$  turn (Pro<sup>5</sup>) has its carbonyl carbon eclipsed with the  $\text{C}_\beta$  methylene of the proline ring, resulting in an unusually high field chemical shift frequency for the  $\text{C}_\beta$  resonance<sup>24</sup> in solution and the solid state. The other proline (Pro<sup>2</sup>) is in the  $\beta$  turn and has a  $\text{C}_\beta$  resonance that is significantly downfield from that of Pro<sup>5</sup>. Because of the invariance of  $\text{C}_\beta$  resonance positions  $\Delta\delta_{\beta\gamma}$ , the difference in chemical shift between the  $\text{C}_\beta$  and  $\text{C}_\gamma$  resonances serves as a convenient conformational marker in these peptides. This parameter is large ( $\sim 4$  ppm) for a proline in a  $\beta$  turn and small ( $\leq 1$  ppm) for a proline in a  $\gamma$  turn.

The  $^{13}\text{C}$  NMR spectra of crystalline cyclic (D-Phe-Pro-Gly-D-Ala-Pro) at 3.5 T (Figure 1A) and at 5.9 T (Figure 1B) fields have well-resolved methyl, methylene, and aromatic resonances that are very similar in frequency and line width to those observed in solution. Resonances from carbons directly bonded to nitrogens differ significantly in appearance in the spectra obtained at 3.5- and 5.9-T fields. This is particularly clear for the carbonyl carbon (160–180 ppm) and  $\alpha$  carbon (45–65 ppm) resonance regions. At the higher field strength the apparent spectral resolution is

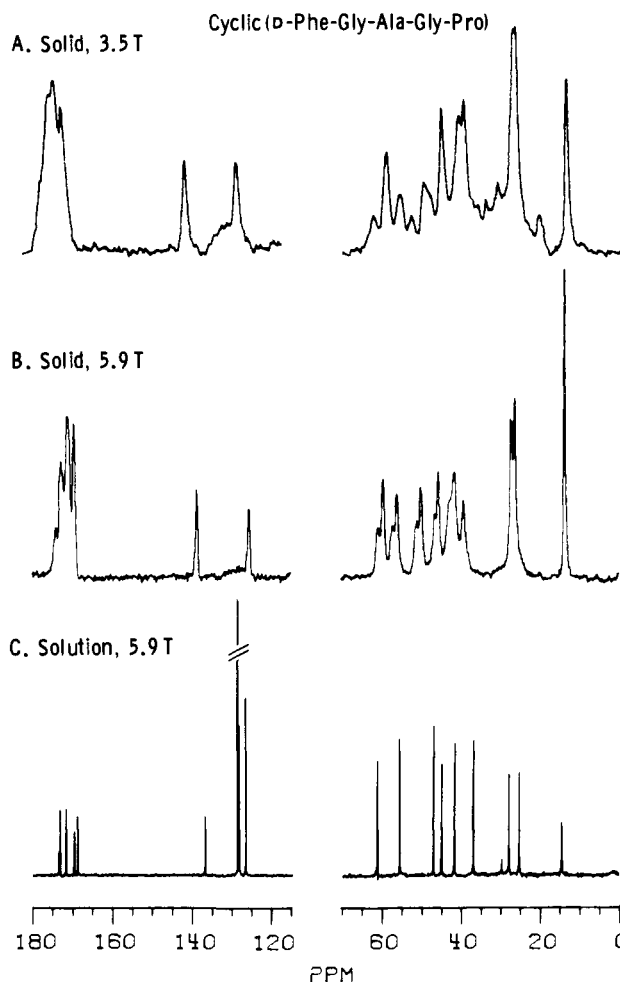
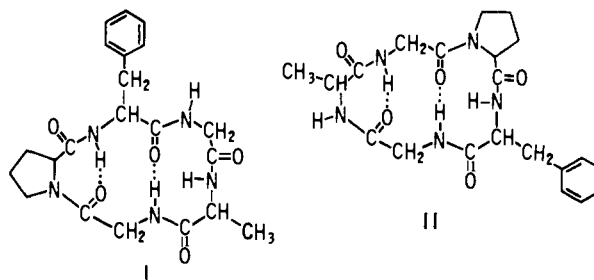


**Figure 2.**  $^{13}\text{C}$  NMR spectra of cyclic (D-Phe-Gly-Ala-Gly-Pro). (A) Solid-state NMR spectrum at 3.5 T obtained with 16 000 single cross-polarization acquisitions with 2.5-mT decoupling, 3-s recycle delay, and 3.9-kHz spin rate in a Delrin rotor. (B) Solid-state NMR spectrum at 5.9 T obtained with 4000 single cross-polarization acquisitions with 1.5-mT decoupling, 20-s recycle delay, and 3.9-kHz spin rate in a Delrin rotor. (C) Solution spectrum at 5.9 T of a 10-mg/mL  $\text{CDCl}_3$  solution.

substantially better, because the  $^{14}\text{N}$ -induced splitting and broadening of the  $^{13}\text{C}$  resonances is decreased at higher fields.<sup>6</sup>

**(2) Cyclic (D-Phe-Gly-Ala-Gly-Pro).** The  $^{13}\text{C}$  NMR spectra of cyclic (D-Phe-Gly-Ala-Gly-Pro) in Figure 2 are distinctive in several respects. Both conformational and dynamical effects strongly influence the appearance of the spectra. At first glance, there are almost no similarities between the solution and solid-state  $^{13}\text{C}$  NMR spectra of this peptide. The carbonyl and  $\alpha$  carbon resonance regions in the solid-state NMR spectra clearly show the splittings and broadenings induced by the bonded nitrogens. The difference in apparent resolution in the  $\alpha$  carbon resonance region (45–65 ppm) between the spectra obtained at 3.5 and 5.9 T is particularly impressive for cyclic (D-Phe-Gly-Ala-Gly-Pro). Spectra at the resolution of that in Figure 2B suggest that a detailed analysis of the nitrogen-induced splitting for all carbon sites in a peptide backbone can be used for detailed conformational analysis of secondary structure. There is a large difference in the

(21) Lee, M.; Goldberg, W. I. *Phys. Rev.* **1962**, *128*, 2042–2053.

(22) Matthews, H. R.; Matthews, K. S.; Opella, S. J. *Biochem. Biophys. Acta* **1977**, *497*, 1–13.

(23) Karle, I. L. In "Perspectives in Peptide Chemistry"; Eberle, A., Geiger, R., Wieland, T., Eds.; Karger: Basel, 1981; pp 261–271.

(24) Siemion, I. Z.; Wieland, T.; Pook, K. H. *Angew. Chem.* **1975**, *87*, 712–714.

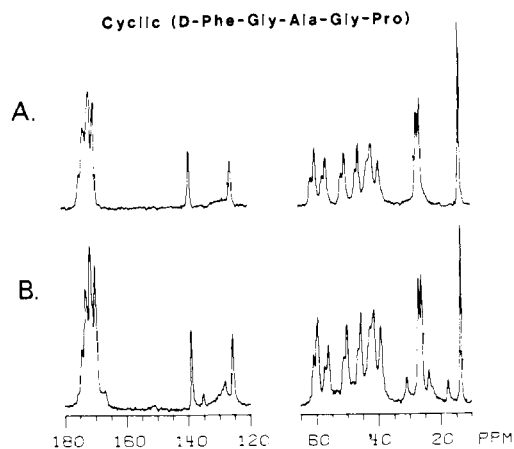


**Figure 3.**  $^{13}\text{C}$  solid-state NMR spectra of cyclic (D-Phe-Gly-Ala-Gly-Pro) at 5.9 T as in Figure 2. (A) Recrystallized slowly from methanol. (B) Recrystallized rapidly from methanol.

$\Delta\delta_{\beta\gamma}$ , proline shifts for the solution and solid-state spectra of cyclic (D-Phe-Gly-Ala-Gly-Pro). The solution spectrum (Figure 2C) indicates that the molecule is probably undergoing averaging between conformations I and II of Figure 2, with the proline residue in either a  $\beta$  or a  $\gamma$  turn based on a midrange (2.5 ppm) value for the  $\Delta\delta_{\beta\gamma}$  parameter. The solid-state NMR spectra indicate that the proline is in a  $\gamma$  turn in the crystalline sample used for the A and B spectra of Figure 2 because of the small  $\Delta\delta_{\beta\gamma}$  of 0.7 ppm observed.

Samples of the peptide cyclic (D-Phe-Gly-Ala-Gly-Pro) crystallized in two different ways give the  $^{13}\text{C}$  NMR spectra of Figure 3. The proline conformation determined from the  $\Delta\delta_{\beta\gamma}$  parameter in the spectra in Figures 2A,B and 3A is at variance with that recently determined from the crystal structure of this peptide.<sup>25</sup> The spectra in Figure 3 show strong evidence that the peptide can exist in two different conformations, since a physically homogeneous polycrystalline sample gives the well-resolved spectrum in Figure 3A and a sample that appears to be heterogeneous gives the spectrum in Figure 3B with multiple lines in the aromatic (120–140 ppm) and aliphatic spectral regions (10–35 ppm). Although we were unable to obtain samples for NMR spectroscopy with only the second conformational form of the peptide present, some features of the spectrum in Figure 3B, especially the shifts of the second set of proline  $\text{C}_\beta$  and  $\text{C}_\gamma$  resonances, suggest that the same structure of the peptide found in single crystals by X-ray diffraction may be present.

**B. Dynamics.** The aromatic region (120–140 ppm) of the solid-state  $^{13}\text{C}$  NMR spectra of cyclic (D-Phe-Gly-Ala-Gly-Pro) has very unusual patterns. The  $\gamma$  and  $\xi$  carbon resonances of the single phenylalanine in the peptide give sharp single lines; however, the  $\alpha$  and  $\beta$  carbons give rise to a broad ill-defined resonance between the  $\gamma$  and  $\xi$  carbon resonances. This broad resonance intensity can be explained by the phenyl ring in cyclic (D-Phe-Gly-Ala-Gly-Pro) undergoing intramolecular reorientation about the  $\text{C}_\beta$ – $\text{C}_\gamma$  bond axis on a time scale ( $10$ – $10^2$  Hz) that results in intermediate exchange broadening of the isotropic chemical shift resonances. This explanation is consistent with the  $\text{C}_\gamma$  and  $\text{C}_\xi$  resonances being unaffected by the motional process. These aromatic ring resonances contrast greatly with those observed for the cyclic (D-Phe-Pro-Gly-D-Ala-Pro) peptide in Figure 1. There is a reproducible loss of aromatic resonance intensity on going from 3.5 to 5.9 T, indicating that the somewhat larger resonance frequency differences at the higher field are closer to the frequency of ring motions.

In order to explore the influence of inter- vs. intramolecular factors on ring dynamics,  $^{13}\text{C}$  NMR spectra of the peptide cyclic (D-Phe-Gly-Val-Gly-Pro) were obtained. The  $^{13}\text{C}$  NMR spectra of the three peptides discussed in this paper are compared in Figure 4. The aromatic ring dynamics of the peptides with Val and with

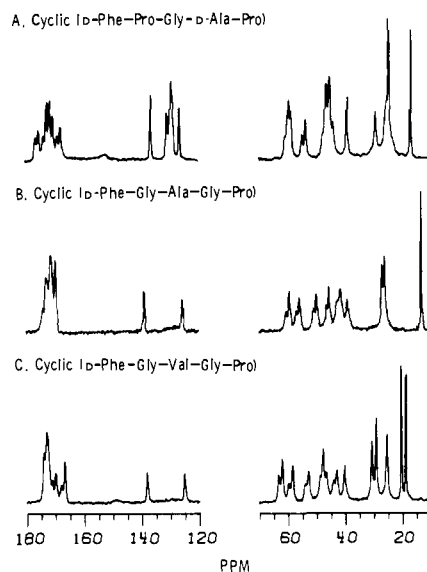


**Figure 4.**  $^{13}\text{C}$  solid-state NMR spectra of cyclic pentapeptides at 5.9 T with the same data and parameters as in Figures 1B and 2B: (A) cyclic (D-Phe-Pro-Gly-D-Ala-Pro); (B) cyclic (D-Phe-Gly-Ala-Gly-Pro); (C) cyclic (D-Phe-Gly-Val-Gly-Pro).

Ala at position 3 are similar, based on the appearance of the aromatic carbon resonances. However, there are differences in the Pro  $\text{C}_\beta$  and  $\text{C}_\gamma$  resonance positions. Otherwise, the resolution of aliphatic resonances and the influence of  $^{14}\text{N}$  on the spectra of these peptides are similar.

The dynamics of phenylalanine and tyrosine rings have been studied in the free amino acids, peptides containing these residues, and proteins containing these residues by solid-state NMR.<sup>13,26–33</sup> The main approach has been to label these rings with  $^2\text{H}$  and record the  $^2\text{H}$  NMR spectra. The line shapes of the powder patterns from the  $^2\text{H}$  quadrupole interaction are altered significantly by intramolecular motions. Rings undergoing two-site flip motions are readily differentiated from those that undergo diffusional rotations or are rigid. Complementary powder pattern line-shape analyses are possible for  $^{13}\text{C}$  chemical shift anisotropy and  $^{13}\text{C}$ – $^1\text{H}$  dipole–dipole couplings.<sup>28,33</sup>

The high-resolution  $^{13}\text{C}$  NMR spectra of these cyclic peptides indicate that two of them have ring motions on the  $10$ – $10^2$  Hz time scale. The  $^{13}\text{C}$ ,  $^2\text{H}$ , and corresponding simulated NMR spectra for cyclic (D-Phe-Gly-Ala-Gly-Pro) and cyclic (D-Phe-Gly-D-Ala-Pro) are in Figure 5. These peptides were synthesized with Phe- $d_3$  to label the phenylalanine side chains. The  $^2\text{H}$  NMR powder patterns for both peptides show the rings to be rigid on the  $10^6$ – $10^7$  Hz time scale of the  $^2\text{H}$  quadrupole interaction. Therefore, the phenyl ring in cyclic (D-Phe-Gly-Ala-Gly-Pro) is rigid on the basis of a spin interaction that is sensitive to rapid motions and is mobile on the basis of a spin interaction that is sensitive to relatively slow motions. Similar behavior has been seen for phenylalanine hydrochloride.<sup>28</sup> On the basis of definitive

(26) Gall, C. M.; DiVerdi, J. A.; Opella, S. J. *J. Am. Chem. Soc.* **1981**, *103*, 5039–5043.

(27) Gall, C. M.; Cross, T. A.; DiVerdi, J. A.; Opella, S. J. *Proc. Natl. Acad. Sci. U.S.A.* **1982**, *79*, 101–105.

(28) Frey, M. H.; DiVerdi, J. A.; Opella, S. J. *J. Am. Chem. Soc.*, in press.

(29) Kinsey, R. A.; Kintanar, A.; Oldfield, E. *J. Biol. Chem.* **1981**, *256*, 9028–9036.

(30) Schramm, S.; Kinsey, R. A.; Kintanar, A.; Rothgeb, T. M.; Oldfield, E. *Biomolecular Stereodynamics II* **1981**, 271–286.

(31) Rice, D. M.; Wittebort, R. J.; Griffin, R. G.; Meirovitch, E.; Stimson, E. R.; Meinwald, Y. C.; Freed, J. H.; Scheraga, H. A. *J. Am. Chem. Soc.* **1981**, *103*, 7707–7710.

(32) Rice, D. M.; Blume, A.; Herzfeld, J.; Wittebort, R. J.; Huang, T. H.; Das Gupta, S. K.; Griffin, R. G. *Biomolecular Stereodynamics II* **1981**, 255–270.

(33) Schaefer, J.; Stejskal, E. O.; McKay, R. A.; Dixon, W. T. *J. Magn. Reson.* **1984**, 85–92.

(34) Maricq, M. M.; Waugh, J. S. *J. Chem. Phys.* **1979**, *70*, 3300–3316.

(25) Karle, I. L., unpublished results.

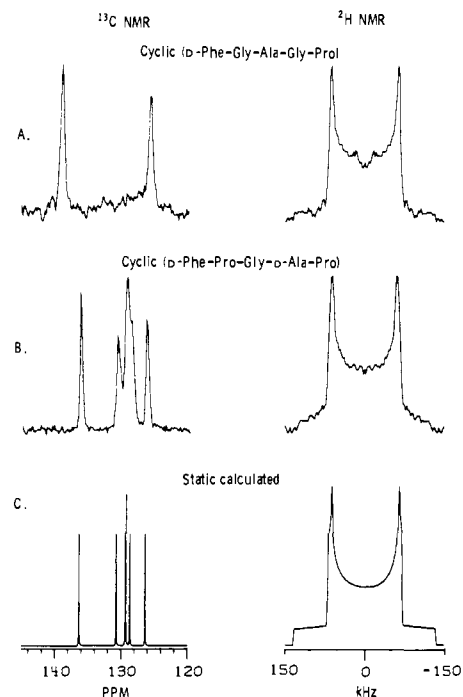


**Figure 5.**  $^{13}\text{C}$  and  $^2\text{H}$  solid-state NMR spectra of the aromatic rings of cyclic peptides. The  $^{13}\text{C}$  NMR spectra were obtained as described for Figures 1 and 2. The  $^2\text{H}$  NMR spectra were obtained with a quadrupole echo pulse sequence of Phe- $d_5$  labeled peptides with an interpulse spacing of  $50\ \mu\text{s}$  and a recycle delay of  $60\ \text{s}$ : (A) cyclic (D-Phe-Gly-Ala-Gly-Pro); (B) cyclic (D-Phe-Pro-Gly-D-Ala-Pro); (C) arbitrary  $^{13}\text{C}$  chemical shift "stick" spectrum for a rigid ring and a calculated  $^2\text{H}$  NMR powder pattern for a rigid ring.

results for phenyl rings undergoing faster motions, the reorientation of the phenyl ring in cyclic (D-Phe-Gly-Ala-Gly-Pro) is probably a twofold flip process. The phenyl ring in cyclic (D-Phe-Pro-Gly-D-Ala-Pro) is rigid on both the slow and fast time scales of these experiments. A more detailed analysis is necessary to describe any small amplitude motions that may be present in these rings.

**C. N-H Bond Lengths.** The dipole-dipole interaction can be used to measure bond lengths because it has an  $r^{-3}$  dependence on the distance between nuclei.<sup>9</sup> The N-H bond lengths are of particular interest in molecules where hydrogen bonding occurs. The two reverse turns in cyclic (Gly<sup>1</sup>-D-Pro<sup>2</sup>-Gly<sup>3</sup>-Ala<sup>4</sup>-D-Pro<sup>5</sup>) are stabilized by intramolecular hydrogen bonds as illustrated in Figure 6. X-ray diffraction results<sup>23</sup> on this peptide show substantial differences in the geometries of the peptide bonds involved in the intramolecular hydrogen bonds, with a  $19^\circ$  nonplanarity of the Pro<sup>2</sup>-Gly<sup>1</sup> bond and an essentially planar Gly<sup>3</sup>-D-Ala<sup>4</sup> bond. The nitrogens of Gly<sup>1</sup> and Ala<sup>4</sup> were labeled with  $^{15}\text{N}$  synthetically. Because the isotropic chemical shifts of the two nitrogen resonances are well separated, the dipolar couplings for both sites could be measured with  $^{15}\text{N}/^1\text{H}$  separated local field spectroscopy in the same sample with the same data sets in order to avoid relative experimental errors.

Figure 6 contains the two-dimensional contour plots of the magic angle sample spinning  $^{15}\text{N}-^1\text{H}$  separated local field experiment. Single resonance lines are seen in the chemical shift dimension, since the spinning is rapid compared to the  $^{15}\text{N}$  chemical shift tensor for amide sites. Spinning sidebands are seen in the dipolar dimension because the spinning is slow compared to the magnitude of the  $^{15}\text{N}-^1\text{H}$  dipole-dipole couplings. The sideband intensities are directly related to the frequency breadth of the underlying powder patterns.<sup>32</sup> The experimental sideband intensities for slices through the centers of the two nitrogen resonances are shown at the bottom of Figure 6. The dipolar powder patterns calculated from the experimental sideband intensities are above each slice. The frequency breadth between the discontinuities of the powder patterns is a direct measure of

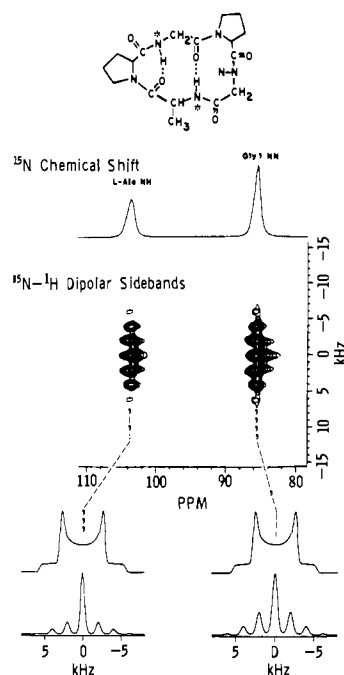


**Figure 6.**  $^{15}\text{N}/^1\text{H}$  two-dimensional dipole-dipole/chemical shift spectrum of cyclic ( $^{15}\text{N}$ -Gly-D-Pro-Gly- $^{15}\text{N}$ -Ala-D-Pro) obtained at 3.5 T with 1.5-mT decoupling and a 2.0-kHz spin rate from 64  $t_1$  values. Top:  $^{15}\text{N}$  chemical shift spectrum. Middle: contour plot of chemical shift vs. heteronuclear dipolar sidebands. Bottom: slices through center of contours for the two nitrogen sites and the reconstructed powder patterns based on the sideband intensities.

the magnitude of the N-H dipolar coupling and the associated bond length.<sup>9</sup> The Ala<sup>4</sup> N-H bond length is  $1.07 \pm 0.05\ \text{\AA}$  and the Gly<sup>1</sup> N-H bond length is  $1.10 \pm 0.05\ \text{\AA}$ , based on the data of Figure 6. We interpret these two bond lengths to be the same within experimental error.

## Discussion

The results presented in this paper emphasize comparisons among similar peptides and sites and between samples in solution and the solid state. These results demonstrate that fundamental spectroscopic experiments can be carried out on biological molecules with sufficient complexity to have interesting properties. The nuclear spin interactions at specific peptide sites, especially when isotopic labeling is employed, can be analyzed at the same level of detail obtained in studies of these interactions in the simplest of model systems. Depending on the site, spins, interactions, and experimental design, both structural and dynamical features of peptides can be described explicitly.

High-resolution spectroscopy is possible in the solid state for these molecules, and useful chemical shift comparisons can be made among the various  $^{13}\text{C}$  resonances. The effects of  $^{14}\text{N}$  on the  $^{13}\text{C}$  resonances appear throughout, and the spectra obtained at 5.9 T show nearly complete resolution of the nitrogen-induced splittings of the  $\alpha$ -carbon resonances. While poorer resolution of these characteristic splittings is seen in the carbonyl resonance region in these one-dimensional chemical shift spectra, recent two-dimensional studies show that complete resolution can be obtained for these resonances.<sup>12</sup> The measurement of both  $\alpha$  and carbonyl carbon resonance splittings from individual amide nitrogens enhances the prospects for the  $^{14}\text{N}$ -induced  $^{13}\text{C}$  splittings being useful in conformational analysis of peptides.

Striking evidence of ring motions is seen in the  $^{13}\text{C}$  NMR spectra of some cyclic pentapeptides. The use of  $^2\text{H}$ -labeled peptides enables the ring dynamics to be more fully characterized.

The measurement of N-H bond lengths through the heteronuclear dipole-dipole interactions is possible. These bond lengths can help to characterize the hydrogen bonds in these peptides.

Several specific conclusions were reached concerning the cyclic pentapeptides studied. The isotropic  $^{13}\text{C}$  chemical shifts are

consistent in showing that cyclic (D-Phe-Pro-Gly-D-Ala-Pro) exists in the same single conformation in solution and in the solid state but that cyclic (D-Phe-Gly-Ala-Gly-Pro) appears to crystallize in two different forms under some conditions that may be in dynamic equilibrium in solution. The phenyl rings of crystalline cyclic (D-Phe-Gly-Ala-Gly-Pro) and cyclic (D-Phe-Gly-Val-Gly-Pro) undergo relatively slow ( $10\text{--}10^2$  Hz) reorientation about the  $C_\beta\text{--}C_\gamma$  bond axis, although the ring of (D-Phe-Pro-Gly-D-Ala-Pro) is static on this time scale. The N-H bond lengths for the two

different groups involved in intramolecular hydrogen bonds in cyclic (Gly-Pro-Gly-D-Ala-Pro) appear to be quite similar.

**Acknowledgment.** This research is being supported by grant GM-29754 from the N.I.H. S.J.O. is a Senior Fellow at Smith, Kline, and French Laboratories. M.H.F. was supported by a Cell and Molecular Biology Training Grant.

**Registry No.** Cyclic (D-Phe-Pro-Gly-D-Ala-Pro), 75929-66-7; cyclic (D-Phe-Gly-Ala-Gly-Pro), 75929-67-8.

## Conformations, Possible H Bonding, and Microwave Spectrum of 3-Buten-2-ol

Zuzana Smith, Norberto Carballo,<sup>1</sup> E. Bright Wilson,\* Karl-Magnus Marstokk, and Harald Møllendal

Contribution from the Departments of Chemistry, Harvard University, Cambridge, Massachusetts 02138, and the University of Oslo, P.O. Box 1033, Blindern, N-0315 Oslo 3, Norway. Received September 27, 1984

**Abstract:** The microwave spectra of 3-buten-2-ol,  $\text{CH}_2=\text{CHCH}(\text{OH})\text{CH}_3$ , and  $\text{CH}_2=\text{CHCH}(\text{OD})\text{CH}_3$  have been investigated in the 18.0–40 GHz region. More than two conformations are believed to be present; however, the spectra of only two have been assigned. In conformer I the methyl carbon atom and the oxygen atom are in *skew* positions relative to the double bond. The methyl carbon is about  $118^\circ$  from the *syn* position while the oxygen is about  $-122^\circ$  from the *syn* position. The OH hydrogen is roughly *anti* to the methyl group. In conformer II the oxygen atom is about  $+4^\circ$  from the *syn* position with respect to the double bond and the methyl group is about  $+124^\circ$  from the *syn* position. The hydroxylic hydrogen is approximately *anti* to the hydrogen on carbon two. In both conformers the hydroxylic hydrogen is close to the double bond, so that it is possible that there is a hydrogen bond between the  $\pi$  electrons and the OH group. The dipole moment components of I have been determined from Stark-effect measurements: they are  $|\mu_a| = 1.30$  (1) D,  $|\mu_b| = 0.3$  (1) D,  $|\mu_c| = 0.47$  (7) D, and  $|\mu_{\text{tot}}| = 1.41$  (2) D. Rotational constants of three vibrationally excited states of I and the differences in the rotational constants  $A\text{--}C$  and  $\kappa$  of two vibrationally excited states of II are reported, which presumably all belong to the excited C-C torsion. Relative intensity measurements gave the energy difference between the lowest levels of I and II to be 520 (140) cal/mol with I below II. The lowest vibrational frequencies were 91 (19)  $\text{cm}^{-1}$  (I) and 138 (53)  $\text{cm}^{-1}$  (II). A vapor-phase infrared spectrum shows two peaks, one at 3645  $\text{cm}^{-1}$  and the other at 3657  $\text{cm}^{-1}$ , assigned to two OH stretching frequencies.

It has been suggested<sup>2</sup> that molecules containing the chain  $\text{C}=\text{C}\text{--}\text{C}\text{--}\text{O}\text{--}\text{H}$  may be able to form an internal hydrogen bond between the hydroxylic hydrogen and some part of the  $\text{C}=\text{C}$  double bond. Information about such bonding has been sought from electron-diffraction, infrared, and Raman spectra and other techniques. The most certain quantitative method is microwave spectroscopy which, however, has been applied to only a few such molecules.<sup>3–6</sup> The species 3-buten-2-ol has been studied in order to extend this list.

A considerable number of molecules with the  $\text{C}=\text{C}\text{--}\text{C}\text{--}\text{X}$  group occur with the skew or *syn* configuration<sup>7</sup> (see Figure 1, a–c). The anti planar structure is rare (Figure 1, d–f). Table I lists some molecules containing this chain whose conformation has been determined by microwave spectroscopy. It has been pointed out<sup>9a</sup> that the skew form is favored by more bulky groups X. Table I also suggests that a hydrogen bond may make the skew form more stable.

The above results for single substitutions indicate that when the chain is of the form  $\text{C}=\text{C}\text{--}\text{CH}(\text{OH})\text{CH}_3$  steric effects might lead to the energy order H *syn* lowest, OH *syn* second lowest, and  $\text{CH}_3$  *syn* third lowest (see Figure 1, b, c, a). However, the relative energies of OH and  $\text{CH}_3$  in the *syn* position are not certain because of the possible effect of hydrogen bonding.

The orientation of the hydroxyl hydrogen with respect to the C–C bond (rotation around the C–O bond) is less firmly predicted. In the absence of H bonding one normally expects the H in OH

**Table I.** Conformations of Related Molecules Determined by MW Spectroscopy

	% skew	% <i>syn</i>	ref
1-butene	83	17	8
$\text{CH}_2=\text{CHCH}_2\text{F}$	60	40	9
$\text{CH}_2=\text{CHCH}_2\text{Cl}$	84 <sup>a</sup>	16 <sup>a</sup>	10
$\text{CH}_2=\text{CHCH}_2\text{Br}$	100		11
$\text{CH}_2=\text{CHCH}_2\text{I}$	100		12
$\text{CH}_2=\text{CHCH}_2\text{OH}$	<100		3
$\text{CH}_3\text{CH}_2=\text{CHCH}_2\text{OH}$	100 <sup>b?</sup>		4
$\text{CH}_2=\text{C}=\text{CHCH}_2\text{OH}$	~100		6

<sup>a</sup> The population was determined with infrared spectroscopy<sup>10b</sup> and NMR<sup>10c</sup> spectroscopy. <sup>b</sup> From low-resolution MW which might not show other conformers.

to be staggered ( $\pm$  *gauche* or *anti*) with respect to the three bonds at the other end of the O–C axis, but if a hydrogen bond is indeed

(1) Present address: Department of Chemistry, University of Wisconsin, Madison, WI 53706.

(2) (a) Von Luttke, W.; Mecke, R. *Z. Elektrochem.* **1949**, *53*, 24–249. (b) Oki, M.; Iwamura, M.; Urushibara, Y. *Bull. Chem. Soc. Jpn.* **1958**, *31*, 769–770. Part I of the spectroscopic series: Studies of Intramolecular Interaction between Hydroxyl Group and  $\pi$ -Electrons. (c) Schleyer, P. v. R.; Trifan, D. S.; Bacskai, R. *J. Am. Chem. Soc.* **1958**, *80*, 6691–6692.

(3) Murty, A. N.; Curl, R. F., Jr. *J. Chem. Phys.* **1967**, *46*, 4176–4180. (4) Lum, D. K.; Bauman, L. E.; Malloy, T. B., Jr.; Cook, R. L. *J. Mol. Struct.* **1978**, *50*, 1–6.

(5) Marstokk, K.-M.; Møllendal, H. *Acta Chem. Scand.* **1981**, *A35*, 395–401.

\* Address correspondence to this author at Harvard University.